

THE AERODYNAMIC DEVELOPMENT  
OF THE FOKKER 100

E. Obert  
Chief Advanced Design Engineer \*  
Fokker Aircraft B.V.  
Amsterdam, The Netherlands

ABSTRACT

An overview is presented of the aerodynamic design of the Fokker 100. The development of the aircraft geometry, in particular that of the wing, is described in detail starting from the F28. The estimated performance characteristics such as cruise drag, buffet-onset boundary and maximum lift coefficient are compared with flight test data.

Finally some stability and control characteristics are described, both as pre-flight estimates and as found on the actual aircraft.

INTRODUCTION

The development of any aircraft is an evolutionary process which leads in many cases to a final product considerably different from the initial concept. To the uninitiated the path along which this development process proceeds may give the impression of being full of seemingly unnecessary winding turns.

This illustrates however the complexity of modern civil transport aircraft where every decision is a compromise between often highly conflicting requirements which themselves tend to change during the design period.

The Fokker 100, with its formal designation Fokker F-28 Mk0100, fared no differently. When the first ideas about what was to become the Fokker 100 were formulated in 1982 these were triggered by the following:

1. Strong indications existed that in the European Community after 1987 newly built aircraft would have to comply with the noise requirements of ICAO Annex 16 Ch. 3, comparable to FAR 36, Stage III.
2. The market required aircraft with a larger payload capacity than the 85 seats of the F-28 Mk4000.
3. In view of the operating environment the economics, in particular the fuel economics had to be improved.

The latter were of particular significance for the F-28. Since its initial certification the F-28 MTOW had risen from 56700 lb to 73000 lb. The measures taken to decrease climb and cruise drag over that period had been limited to a single 2 x 0.75 m span extension. Engine development had been limited to a single increase in thrust of 4% in hot-and-high conditions.

When the F-28 was originally conceived in 1961-'62 an important market was seen among the smaller less sophisticated operators. Consequently, a major design requirement for the F-28 was that the flight handling characteristics and the degree of system complexity should be such that transition from say a DC-3 to an F-28 would not pose any problems, both for pilots and the maintenance crew. In particular the transonic characteristics should be very docile, also in the light of a number of incidents and accidents which occurred at that time to first-generation civil jet aircraft due to severe turbulence or system failures which caused speed increases up to or above  $M_D$ .

In view of the above it was decided that no Mach-trim compensator would be considered and that the absence of high-speed pitch-up or tuck-under tendencies should be obtained entirely through aerodynamic design.

This goal was achieved although at a price. In order to obtain the required transonic pitching moment characteristics a fairly thick airfoil section at 40% half span was selected with a rather high leading-edge suction peak in the design condition. This was to ensure that above  $M_{Mo}$  the spanwise distribution of flow separation and lift break-down and changes in the downwash conditions at the tailplane occurred according to a predetermined pattern.

Initially these high local superelevations did not show any adverse side-effects. As the F-28 was originally designed for MTOW = 54000 lb and a cruise altitude of 25000 ft (the maximum altitude was 30000 ft) the design lift coefficient had the modest value  $C_L = 0.20$  at  $M = 0.73$ . The final F-28 version had a MTOW = 73000 lb and a maximum cruise altitude of 35000 ft leading to  $C_L = 0.45$  at  $M = 0.73$  at that altitude had the engine thrust been available.

At this extreme flight condition the transonic drag increase on the original F-28 wing is not insignificant and when, in early 1982, serious discussions started between Rolls-Royce, Gulfstream and Fokker on the development of a re-fanned Spey engine, it was felt that all primary ingredients existed for a major development effort on a new project.

\* Former Head Aerodynamics and Performance Dept.

Copyright © 1988 by ICAS and AIAA. All rights reserved.

## THE FOKKER 100 - A SHORT DEVELOPMENT HISTORY

In the first months of 1982 a study was performed into the various options available, including the design of a completely new wing, for a new F-28 version. The study showed that the most attractive approach would be to stay with the basic components of the aircraft but to modify each component extensively.

The first design specification of Project 332 (June 1982) showed:

MTOW = 84500 lb  
MLW = 80200 lb  
MZFW = 71000 lb

for a payload of 100 passengers at 32 in. seat pitch and a range of 950 nm.

The fuselage was lengthened by 114.8 in. in front of the wing and by 67.1 in. aft of the wing.

The wing shape envisaged for the project was identical to wing 4 in the windtunnel programme.

In the Type Specification dated 15 February 1988 the weights are:

MTOW = 95000 lb  
MLW = 85500 lb  
MZFW = 77500 lb

for a payload of 107 passengers at 32 in. seat pitch and a range of 1310 nm.

A further weight growth step to 98000 lb will be certificated shortly. The fuselage has been lengthened, relative to the F-28 Mk4000, by 144.1 in. in front of the wing and by 82.0 in. aft of the wing. Also, the wing reference area went up from 940.2 sq.ft. to 1006.5 sq.ft. Figure 1 shows a three-view of the final Fokker 100 configuration.

This growth in weight and size required an increase in engine thrust from the original static thrust of 12550 lb SL, ISA for the original Tay via 13850 lb for the Tay 620 to 15150 lb for the Tay 650.

Table I presents some further data on characteristics which have gradually developed during the design process.

Apart from a considerably larger payload-range capability than originally envisaged, another originally unanticipated development was the incorporation right from the start of a highly sophisticated avionics package including CAT 3B autoland capability. Market requirements necessitated this development allowing however a check right from the first flight on the proper interfacing between control surface and AFCAS operation.

Finally, the flight tests showed that the efforts to produce low internal and external noise levels on the Fokker 100 were extremely successful. The aircraft has set new standards for combined interior and far field noise levels. (Figures 2 and 3). In today's noise-sensitive operating environment this is extremely important in order to make full use of successful aerodynamic design for performance.

## WINDTUNNEL TEST PROGRAMME

The computer codes used in the design computations which produced the Fokker 100 geometry have been described in ref. 1.

The windtunnel test programme was performed on the following models:

1. A 1:20 scale complete model tested in the High Speed Tunnel (HST) of NLR in Amsterdam. This model, due to its modular build-up, could be tested in many configurations. Because the HST can be operated from  $M = 0$  up to Mach numbers above  $M = 1$  at pressures up to 4 atm both the cruise and the take-off and landing configurations with flaps deflected could be tested on this model. Most of the tests were performed at  $Re_c = 3.0$  million.

2. A 1:12 scale half model, also tested in the HST at Reynolds numbers up to 5 million.

3. A two-dimensional model tested in the Low-Speed Tunnel (LST-NOP) of NLR to analyse airfoil section and flap modifications (At Reynolds numbers up to 3 million).

4. A 1:4 scale outer wing model also tested in the LST-NOP to obtain both static and dynamic test data on the new aileron.

5. A complete low-speed model for tests on the thrust-reverser characteristics including re-ingestion. Apart from the re-ingestion tests, which were performed by Rolls-Royce at Hucknall, this model was also tested in the LST-NOP.

The total windtunnel programme, which included:

- 12 wing geometries
- 4 fuselage geometries
- 7 engine nacelle geometries
- 6 pylon geometries
- 3 horizontal tailplane geometries
- 1 vertical tailplane

took only 1928 hrs to complete of which 1272 hrs were in the HST and 656 hrs in the LST. A total of 25 test campaigns were performed over the period November 1981 - August 1984.

Fokker also took part in two test campaigns by Grumman in the Fluidyne test facilities in the USA as part of the engine exhaust nozzle development.

## THE FOKKER 100 WING DEVELOPMENT

The wing shape of the F-28 is basically determined by four wing sections (Section I through IV) between straight generators. On the Mk4000 the tip extension was obtained by extending the generators between Sections III and IV by 0.75 m thus defining a new Section V.

The first analysis of the possible drag improvements on the F-28 wing centered on a configuration with a straight leading edge connecting the leading edges of Sections I and IV. This produced chord extensions at Sections II and III of 8.7 and 5.7 percent respectively. An initial theoretical analysis in the Spring of 1981 and a more thorough analysis with a viscous transonic flow computer code in the Spring of 1982 produced very encouraging results for a modified Section II with the modification limited to the area in front of the wing front spar.

A further study on the characteristics of the root section (Section I) showed that a modest chord extension of 2 percent with an associated modification of its shape in front of the wing front spar could also produce a significant improvement in Mach drag rise. The computed drag curves as a function of Mach number for  $C_1 = 0.5$  are shown in figure 4 both for the original and the modified sections.

Figure 5 compares the pressure distributions on the basic and the modified sections at  $C_1 = 0.4$  and  $M = 0.675$ .

These results were convincing enough to initiate the design and construction of model components for windtunnel testing and in November 1982 the first tests were performed on behalf of Project 332 which was to become the Fokker 100.

Four wing shapes were tested on an F28 model:

- Wing 1 - The basic F-28 Mk1000/2000 wing.
- Wing 2 - The Mk1000 wing with the above mentioned leading edge chord extensions at Sections I, II and III.
- Wing 3 - The basic F-28 Mk3000/4000 wing (which is the Mk1000/2000 wing with 0.75 m span extension per side).
- Wing 4 - This wing is identical to wing 2 except that a wing tip extension of 1.50 m was applied with Section V being identical to Section IV. Two degrees twist was applied to lessen the chance of tip stall.

This windtunnel investigation showed the modifications to be fully effective. However the span increase on wing 4 with its increased taper clearly had a negative effect on the stalling characteristics of the outer wing, at least at windtunnel Reynolds numbers.

Meanwhile, a further theoretical analysis had shown that the Mach drag rise characteristics on the root section could be further improved by additional chord extension. Initially some reluctance to consider such a modification existed in view of possible problems with the wing-fuselage connection. However the data from the analysis of the root sections indicated that a further windtunnel test was warranted. Therefore, in January 1983, a new windtunnel test was performed in which two new wing shapes were investigated, wings 5 and 6. Both had 1.50 m wing tip extensions relative to the wing of the F-28 Mk1000 (wing 1). Section IV had an increased chord, the increase being 1.5 percent, and a modified leading edge in front of the wing front spar in an effort to improve the outer wing stall behaviour. The outer wing leading edge was taken as a straight line determined by the leading edge positions of Sections II and IV. The difference between the two wings was in the root section, wing 5 having a leading-edge chord extension of 5 percent chord and wing 6 of 9 percent chord. Figure 6 shows the improvements found in the windtunnel tests when compared with the data from wings 3 and 4. Contrary to the results from the computations on the root section modifications, the windtunnel test data showed no improvement in drag, when the root chord extension was increased from 5 percent chord to 9 percent.

Although the improvements were significant it was felt that the wing required further development in anticipation of further weight growth. The next development step then was a rearward chord extension combined with a limited amount of rear camber. The new trailing edge was obtained by increasing the root chord of the original F-28 Mk1000 wing and the tip section V on wing 5 rearward by 5 percent chord and connecting these points by a straight line. In the flap region the application of rear camber was limited to the main flap body aft of the flap spar thus maintaining the vane and all flap suspension and drive mechanisms. In the aileron region the complete aileron was translated rearward and given a slight downward deflection such that the aileron trailing edge was in line with the new flap trailing edge. Computed drag rise data and pressure distributions for the kink section (Section II) of this new wing, wing 8 are compared with corresponding data from wing 5 in figure 7.

Equal Mach drag rise curves and upper surface pressure distributions are found when the lift coefficient of the section with modified trailing edge is about 0.2 higher than the section with the original trailing edge.

The modification described above was tested in the windtunnel in May and July 1983 and produced the expected improvements in drag rise characteristics, buffet boundary and low speed maximum lift coefficient. The stalling characteristics however were not yet satisfactory.

A further slight modification on the outboard wing leading edge of wing 5, tested on a complete model equipped with pressure taps and on the first large half model (wing 9) did not show any significant improvements in the stalling characteristics.

At this point a further market analysis had shown that project P332 would stand a much greater chance of success if its payload-range capacity and thus its take-off weight were slightly increased. This together with the increased uncertainty concerning the noise characteristics of this higher-weight aircraft led to the decision to increase the wing span by a further tip extension of 0.75 m on each side, producing a total span extension of 4.50 m relative to the F28 Mk1000 or 3.00 m relative to the Mk4000.

The new wing, wing 10, was obtained by:

1. Maintaining the geometry of wing 8 up to Section III.
2. Moving Section V of wing 8 outwards by 0.75 m while maintaining the straight trailing edge of wing 8.
3. Connecting the leading edges of Sections III and V by a straight line thus producing a wing leading edge with kinks at Sections II and III.
4. Designing a new leading-edge on Section IV in front of the wing front spar such that the wing stalling characteristics would be improved. The leading-edge chord increase of a further 5.3 percent chord on wing 8 produced the degree of freedom in geometry required to obtain a satisfactory leading edge shape.

The definitive wing planform for the Fokker 100 together with the F-28 Mk1000/4000 wing is shown on figure 8. A comparison is also shown between the basic F-28 wing sections and the final definition sections of the Fokker 100 wing (wing 12).

Wing 10, which was tested in November 1983 gave the anticipated improvement in stalling characteristics together with a gain in maximum lift of  $\Delta C_{Lmax} = 0.10$ . However, due to the rather large leading-edge radii on the outer wing sections an unacceptably large drag rise at cruise Mach numbers occurred at low lift coefficients (Figure 9). Therefore a modification to the lower leading edge of Sections III and IV was made in order to lower the suction peak which occurs in this area at high Mach numbers and low lift coefficients. This is illustrated in figure 10. The modified wing, wing 11, was tested in December 1983. Figure 9 shows the effect of the seemingly minor modification.

The outboard wing leading-edge modification on wing 11 had again caused a slight deterioration in stalling characteristics. It was therefore decided to apply a modification to the leading edge of Section II comparable to that on Sections III and IV in order to stimulate initial flow separation at high angles-of-attack on the inboard wing. With this modification, the definitive Fokker 100 wing, wing 12 was tested in the High-Speed Tunnel (HST) at NLR in January 1984. It showed satisfactory characteristics with respect to high- and low-speed drag, pitching-moment, buffet-onset boundary, maximum lift coefficient and stalling behaviour. This result was obtained through 10 development steps (wings 1 and 3 being F-28 wings) over a 15-month windtunnel test period taking 9 test campaigns and 428 tunnel occupancy hours.

In figure 11 a comparison is presented between the pressure distribution at various flight conditions on a representative wing section of the F-28 and the Fokker 100.

The rapidity with which the basic wing development program was executed is almost entirely due to the present state-of-the-art of computer technology with respect to both the hardware and the software. Not only can accurate design and analysis computations be performed quickly but also efficient pre-processing programs allow a fast, accurate and detailed geometry generation which is not only used for the computations but with a minimum of effort can be translated into data fed into the numerically-controlled milling machines producing the new windtunnel model components.

#### DRAG CHARACTERISTICS

The past three decades have shown a large improvement in our understanding of transonic phenomena including the effects of Reynolds number although a number of questions still remain to be answered. The effects of, in particular non-solid, tunnel walls, model suspension and the general level of test equipment accuracy however are still insufficiently known to prevent an occasional feeling of embarrassment when comparing predictions, based on direct windtunnel data or data corrected for known or assumed scale and model test effects, with actual flight test data.

When the F-28 was tested it was found that each version showed a consistent difference in its drag rise characteristics between windtunnel and flight test data. (All windtunnel data except for maximum lift discussed in this paper refer to test conditions with boundary layer transition fixed near the leading edge). The flight test data showed a steeper Mach drag rise than the windtunnel data the difference being most significant at the highest lift coefficients tested. (Figure 12). Remarkably, when in the course of the Fokker 100 design activities the drag of the F-28 was analysed with the computer code XFL022 a very good agreement was found between the computed drag and the flight test data. (Figure 12).

In itself this has only limited meaning because XFLO22 is a non-viscous code and the trailing-edge flow direction is chosen somewhat arbitrarily in order to obtain shock-wave positions in accordance with windtunnel test data. However the result made us wary and in predicting the full-scale Mach drag rise for the Fokker 100 the difference between the windtunnel and flight test data from the F-28 was incorporated, using a somewhat arbitrary scaling rule based on the peak Mach number ahead of the shock wave.

Figure 13 presents a comparison for  $C_L = 0.55$  of the difference in Mach drag rise between the windtunnel test data and the data obtained with XFLO22, the full-scale prediction and the actual flight test data. Note the very good agreement between the latter two. An equally good agreement was found at lower lift coefficients.

A pleasant surprise, if not a sign of true professionalism, came out of the comparison between predicted and measured subsonic drag in the cruise configuration. As the subsonic drag polar turned out to be parabolic (as expected) it is fair to describe it with a "zero-lift drag" term and an induced drag term. The latter is determined by the "Oswald efficiency factor",  $e$ . The "zero-lift" drag coefficient  $C_{D0}$  from the flight tests agreed very well with pre-flight estimates. However, based on F-28 experience and an empirical correlation of flight test data on other aircraft, the pre-flight estimate for the induced drag factor was slightly lower than the average number from the windtunnel tests.

When the flight test data were analysed it turned out that the difference in induced drag factor between windtunnel and flight test data had been estimated correctly. Only it had the opposite sign! (figure 14).

As a consequence in most climb and cruise conditions the induced drag is about 10 percent lower than the pre-flight estimate resulting in a 3 to 4 percent lower overall drag.

#### BUFFET-ONSET BOUNDARY

Simultaneously with the continuing decrease in Mach drag rise through the successive development steps of the Fokker 100 wing the buffet-onset boundary was improved. Figure 15 shows windtunnel test data for the successive wing designs compared to the buffet-onset boundary for the F-28 as obtained from flight tests.

The full-scale estimate for the Fokker 100 was based on windtunnel test data at various Reynolds numbers on both complete models and large half models. As indicated on figure 16 for wing 12 the windtunnel buffet-onset data were then extrapolated to representative full-scale Reynolds-numbers. Figure 17 compares the buffet-onset boundary found in the windtunnel at  $Re = 3$  million with the estimates for the full-scale aircraft based on windtunnel tests, computations with the XFLO22 code and as obtained from flight test data.

#### HIGH-SPEED PITCHING MOMENT CHARACTERISTICS

One of the challenges in the design of a transonic wing is ensuring acceptable pitching moment characteristics once flow separation occurs behind the shockwave. Two particular areas of concern exist:

1. The aircraft characteristics when the buffet-onset boundary is exceeded at cruise Mach numbers.
2. The flight characteristics when  $M_{MO}$  is exceeded.

Figure 18 demonstrates that no pitch-up tendency occurs on the Fokker 100 when the aircraft is taken to angles-of-attack above those for buffet-onset and that the required control force actually increases.

Contrary to the F-28 the Fokker 100 shows, at aft C.G. a mild pitch-up tendency at  $M_D = 0.84$  when the aircraft is accelerated from a trimmed condition at  $M_{MO} = 0.75$  without a stability augmentation device. This pitch-up tendency is mild and easily controllable. However as the airworthiness requirements demand at least neutral stability up to  $M_D$  a single-channel Mach trim compensator is installed. Originally when the aft centre-of-gravity limit in the loading diagram was at 33 percent MAC it was envisaged to operate only above  $M_{MO}$ . When this aft limit was moved to 35 percent MAC the system was made to operate also in the cruise regime. However, the resulting additional control force is so small that a single-channel system could be maintained. Figure 19 shows the pre-flight estimate and the measured stick-force-versus-speed curve both with and without Mach-trim compensator activated.

#### LOW-SPEED MAXIMUM LIFT AND STALLING CHARACTERISTICS

During wing design great care was taken to ensure that the definitive wing for the Fokker 100 would produce the highest possible maximum lift coefficient in order to realise satisfactory field performance without the application of wing slats. Good lateral and longitudinal stability and control in the stall were mandatory in order to make maximum use of the allowable margin between  $V_{S1g}$  and  $V_S$ .

Therefore much attention was given in the basic wing design process to a spanwise variation in leading-edge bluntness such that at high angles-of-attack the highest leading-edge suction peak occurred on the inboard wing. This had been very successful on the F-28. However the much more stringent requirements on the cruise drag for the Fokker 100 made it more difficult to achieve. Figure 20 shows the spanwise variation of the suction peak at high angles-of-attack for successive wing designs. This figure shows clearly the effect of the various leading-edge modifications on the suction peak distribution.

Windtunnel tests on both complete and half-models at Reynolds-numbers up to 5 million showed that, although the successive leading-edge modifications led to improved stall characteristics more had to be done. Various inboard stall-control devices were investigated. The most promising configuration in the windtunnel tests turned out to be a small leading-edge fence at Wing Station 5200. Figure 21 shows its effect on the flow break-down pattern and the resulting effect on the maximum lift coefficient and tail-off pitching moment.

Figure 22 shows how the full-scale tail-off  $C_{Lmax, 1g}$  was estimated from the windtunnel tests without stall control devices. In order to obtain pre-flight estimates for the maximum lift coefficient used for performance calculations for various flap settings the windtunnel data were extrapolated to  $Re = 10$  million. Some penalty is then attached to the addition of the stall control devices ( $\Delta C_L = -0.07$ ). Next a correction on  $C_{Lmax, 1g}$  was applied to incorporate the effect of a (usually negative) tailplane load for trimming at the forward centre-of-gravity. Finally an estimated correction was applied equivalent to the expected difference between  $V_{S1g}$  and  $V_S$ , the formal minimum speed in the stall manoeuvre.

In the flight tests on the Fokker 100 various fences, fence positions and stall breaker strips were investigated. In the end it was concluded that, when maximum lift coefficients and stalling characteristics were considered together the most promising configuration in the windtunnel also gave the best overall results in actual flight tests. Therefore a leading-edge wing fence was installed on the aircraft at WSTA 5200 assisted by a tiny stall breaker strip just inboard of the fence to assure consistency in the aircraft's stalling characteristics.

Figure 23 shows the close agreement between the estimated and the measured maximum lift coefficient for various flight conditions based on minimum speeds in the certification stall manoeuvre.

Note that at take-off flap settings the maximum lift coefficients are comparable to the usable maximum lift coefficients of slatted aircraft as the latter are often  $V_{MU}$ -limited.

In particular the longitudinal behaviour during the stall manoeuvre of rear-engined aircraft with T-tails has to be studied carefully. Today's engineering simulators allow a realistic assessment of the stalling characteristics, including a considerable degree of stall penetration, provided a good aerodynamic model has been implemented:

For this reason extended windtunnel tests up to very high angles-of-attack were performed to provide the test data necessary to construct a detailed aerodynamic model.

The stall is a highly dynamic manoeuvre of which the exact pilot reaction forms an integral part. Furthermore, due to the development of the flow separation pattern and the resulting changes of overall aerodynamic forces and moments Reynolds number effects are very important. This means that test data from static windtunnel tests provide at best only a partial insight into the actual stall behaviour of the real aircraft.

In view of the above it was therefore decided that, to minimize risks, pitching moment curves similar to those of the F-28 should be achieved on the Fokker 100. Figure 26 shows that this could only be realised with a horizontal tailplane which has 0.70 m tip extensions. This increase in tailplane span and area also facilitated the realization of the required most rearward centre-of-gravity position. Therefore the increase in horizontal tailplane span and area was incorporated in the design of the aircraft.

Figure 24 illustrates the good agreement found for the F-28 between flight test and simulator stall manoeuvres after only a minor adjustment of the original aerodynamic model based on a mixture of windtunnel and steady flight test data. Applying similar adjustments, which concerned mostly the post-stall behaviour, to the original estimated full-scale Fokker 100 aerodynamic model produced stall time histories as presented in figure 25. Such data gave the confidence that on the Fokker 100 for comparable  $\alpha$ -rates the overshoot in angle-of-attack during the stall manoeuvre would be similar to that on the F-28.

The stall investigation during flight tests showed that this was indeed the case. The degree of nose-down pitch tendency (as well as the maximum lift coefficient) varied somewhat depending on the size and position of the stall control device. As described before after careful consideration of the test data on the various configurations it was decided to adopt a fence at Wing Station 5200. This position gave a minimal lift loss. At the same time this resulted in an adequate pitch down moment following the stall during slow approaches to the stall as required for maximum lift certification. At very high rates of rotation however, attention by the pilot was required to prevent the aircraft reaching extreme angles-of-attack. It was therefore decided to install a post-stall recovery system. At low  $\alpha$ -rates this system is only triggered when angles-of-attack are reached considerably above that for g-break. Consequently during maximum lift certification tests the post-stall recovery system did not operate in the greater majority of the stalls. At high  $\alpha$ -rates an advance term is introduced in the control law preventing the aircraft from reaching extreme angles-of-attack.

## NACELLE AND PYLON DESIGN

The geometry of the nacelles for the Rolls-Royce Tay engine was designed for application both on the Fokker 100 and the Gulfstream IV nacelles, the latter aircraft having a higher cruise Mach number. In the design of the nacelles the usual requirements were taken into consideration concerning minimum intake drag at various mass flow ratios over the complete operating speed range and the ability to cope with large variations in intake flow angles due to angle-of-attack variations and flap deflections without excessive static or dynamic flow distortions at the compressor face. At the rear of the nacelle the drag was minimized by using the minimum boat-tail angle compatible with the bare engine geometry, thrust reverser design and nozzle area.

An interesting problem occurred concerning the nacelle inclination relative to the fuselage centre-line. Figure 27 shows that increasing the nacelle inclination increased the overall lift of the tail-off configuration and changed the pitching moment in a negative sense. On the aircraft this led, certainly at forward centre-of-gravity positions to a higher negative tailplane lift for trimming purposes. Thus, the lower induced drag of the tail-off configuration was counteracted by the higher tailplane trimdrag. The optimum nacelle position, which on the Fokker 100 turned out to be 1 degree less than in the original theoretical design was found by detailed analysis.

The stub wings or pylons to which the engine nacelles are attached have been shaped such that no supersonic velocities occur anywhere over the complete range of cruise lift coefficients, notwithstanding the adjacent convex fuselage and nacelle walls. This was achieved with the aid of panel method calculations.

## AILERON DESIGN AND LATERAL CONTROL

On the F-28 aerodynamic overhang balances are used on the ailerons. The idea behind this was that the aircraft should have acceptable lateral handling characteristics even in the manual mode after a double hydraulic failure. The low hinge moments, being fairly linear up to maximum aileron deflections allow large aileron deflections in the manual mode notwithstanding the fact that the ailerons in that case are driven solely by flying tabs. (See figure 28) The extra drag resulting from the gap between aileron nose and wing structure was considered insignificant because of the low design lift coefficient and the resultant small pressure difference between upper and lower wing surfaces at the gap location.

When the aft-loaded Fokker 100 wing was investigated it turned out that the additional drag due to the aileron gap was not negligible particularly at the higher lift coefficients. It was therefore decided to change to ailerons with internal aerodynamic balances which produce considerably less drag. (See figure 29).

On both the F-28 and the Fokker 100 the ailerons are the sole means of roll control. Therefore, when the decision was taken to increase the wing span a simulator analysis was performed into the effect of aileron span increase on roll control. It turned out that, in particular in simulated cross-wind landings, the improvement in attitude control due to the longer-span ailerons was quite noticeable. The longer-span ailerons, as depicted in figure 30 were subsequently adopted. Figure 28 shows that these longer-span ailerons with internal aerodynamic balance still achieve, notwithstanding their less linear hinge moments, a reasonable deflection when driven solely by the flying tabs.

Finally, figure 31 shows the peak roll rates achieved in roll manoeuvres during flight tests in the first mode (two hydraulic systems operative), the second mode (one system operative) and in the third (manual), tab-driven mode. The excellent roll control characteristics of the Fokker 100 were demonstrated when, with great precision, fully automatic landings were performed with maximum crosswind velocities of more than 30 knots.

## LONGITUDINAL CONTROL

Much effort was put into the design of the longitudinal control system of the Fokker 100 in order to produce the same crisp and direct control characteristics found on the F-28.

Longitudinal control on the Fokker 100 is by a reversible, dual-channel, booster system in which the control force exercised by the pilot is multiplied by a boost ratio 4.8 before it directly drives the elevator. The elevator has an aerodynamic overhang balance and no tab. The trailing-edge bead which was present on the F-28 was found not to be required on the Fokker 100. This resulted in a very low elevator hinge moment coefficient, (Figure 32) producing, notwithstanding a large centre-of-gravity range (Figure 33), elevator stick-forces comparable to those on the F-28 (Figure 34). Trim changes due to changes in aircraft configuration are also minor and comparable to those on the F-28.

## THRUST REVERSER DESIGN

As the thrust reverser design for the Fokker 100 was Fokker's first venture in this area an extensive windtunnel investigation was performed in an effort to arrive at a thrust reverser configuration which would allow efficient twin and single-engine thrust-reverser operation down to low airspeeds with minimum re-ingestion problems.

The configuration finally selected, incorporates a circular deflector plate ("Chinese fan") (Figure 35), covered by the characteristic bulge on the inboard side of the upper thrust reverser door. This deflector plate considerably lessens the immersion of the rudder in the reverser exhaust flow leading to much improved directional control. (Figure 36). The thrust-reverser cut-off speed is 60 knots and the thrust reverser may routinely be used up to Engine Pressure Ratios equal to 1.20. Higher EPR values up to full power, on both and on a single engine can be applied in an emergency without stability or control problems.

#### SOME FURTHER FLIGHT TEST DATA COMPARED WITH PRE-FLIGHT ESTIMATES

One element which becomes increasingly important in aerodynamic design is the ability of the design team to predict the design's characteristics with maximum accuracy. Not only because of the ever-tightening guarantee requirements but also from the pressure to minimize the flight test and certification period and because true prototypes are no longer built. This means that any modification to the aircraft is felt a long way down the production line.

A recent development which underlines the necessity for accurate prediction of the aircraft's characteristics is the increasing use of simulators to train instructor pilots for new aircraft types.

The success the Fokker design team had in timely producing a sufficiently accurate aerodynamic model of the Fokker 100 is illustrated by the fact that instructor pilots for the first customer were successfully being trained on a Fokker 100 simulator built by CAE three months before the aircraft received its certificate of airworthiness in November 1987.

Figures 37 through 41 provide some further illustrations of the generally good agreement between pre-flight estimates and flight test data which was found for many aircraft characteristics.

#### FLIGHT TEST PROGRAMME

As shown on figures 42 and 43 the development and basic certification flight test programme was performed with three aircraft over a period of 11.5 months and required 1052 flight hours. The fairly steady production of flight hours illustrates the limited amount of modification to the aircraft required as a result of the flight test experience.

#### CONCLUSION

We, at Fokker, do not claim that in the Fokker 100 we have produced an aerodynamic design that in no single area can be surpassed by an all-new design. We do claim however that, given certain financial and commercial constraints and requirements, we have in the Fokker 100, through an excellent combination of aerodynamic, engine and acoustic characteristics, airframe structure, relative simplicity, notwithstanding the very sophisticated avionics, and comfort (few middle seats), an aircraft that can stand comparison with any of its competitors.

#### ACKNOWLEDGEMENT

A formal word of thanks is in place here to the many members of the NLR team who contributed to the aerodynamic development of the Fokker 100. In 1983 when many basic engineering decisions had to be made, their total dedication to maximum progress in model design, construction, tunnel testing and data reduction did much to make the whole initial design effort on the Fokker 100 a speedy process.

Sincere thanks are due to my former colleagues of the Aerodynamics Department not only for doing a fine job on the Fokker 100 but also for their contributions to the preparation of this paper in a period when they had many other, more pressing, matters on their minds.

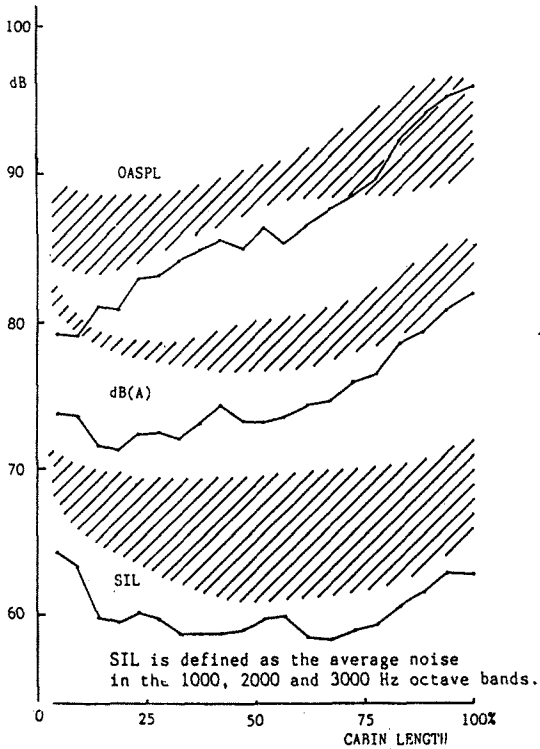
#### References

1. N. Voogt, W.J.A. Mol, J. Stout, D.F. Volkens  
CFD applications in design and analysis of the Fokker 50 and Fokker 100.  
AGARD CP No. 437  
Validation of Computational Fluid Dynamics.  
Lissabon, 2-5 May 1988



	P 332-1 June 1982	P 333-4 July 1983	F28 Mk4000 Febr. 1988
MTOW (lb)	84500	91500	95000 (98000)
MLW (lb)	80200	85000	85500
MZFW (lb)	71000	76500	77500
Fuselage length (ft)	102' 11.6"	106' 5.6"	106' 5.6"
Wing area (sqft)	940.2	1006.2	1006.5
No. of pass at 32"	100	107	107
Range nm	950	1240	1310
Approach speed at MLW (kt)	133	130	129
Engine thrust static, SL, ISA (lb)	12550	13550	13850 (15150)
Take-off field length (SL/ISA + 15°C MTOW)	6000	6700	6725
Initial cruise altitude (ft)	32000	35000	35000
Loading C.G. range	10-35%	7-33%	7-35%

Table I



SIL is defined as the average noise in the 1000, 2000 and 3000 Hz octave bands.

Measured noise levels in

MD 80	30000 ft, Mach .78, average of seatrows
B 737	25000 ft, Mach .78, location unknown
Bae146	25000 ft, 265 kts, aisle position
F28	25000 ft, Mach .73, average of seatrows

— Fokker 100, measured in first production aircraft  
30000 ft, Mach .73, average of seatrows

Figure 2 CABIN NOISE CHARACTERISTICS

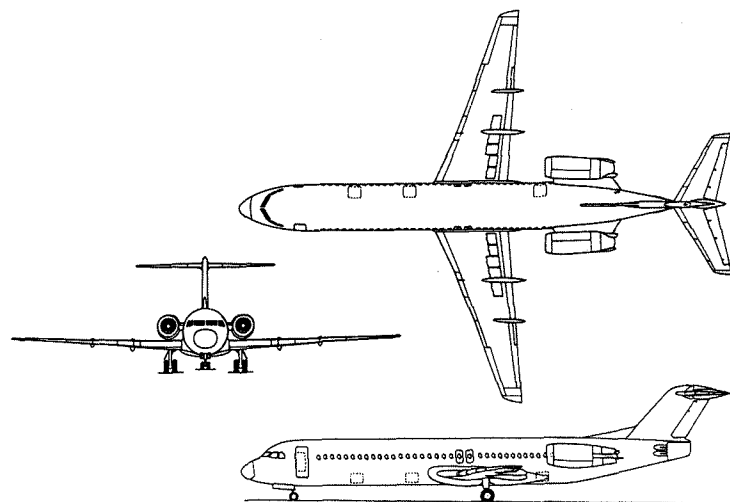


Figure 1 Fokker 100 3-view

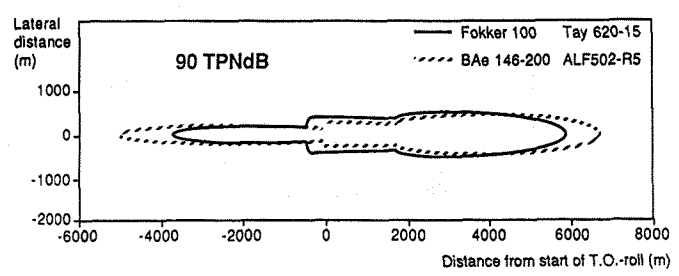
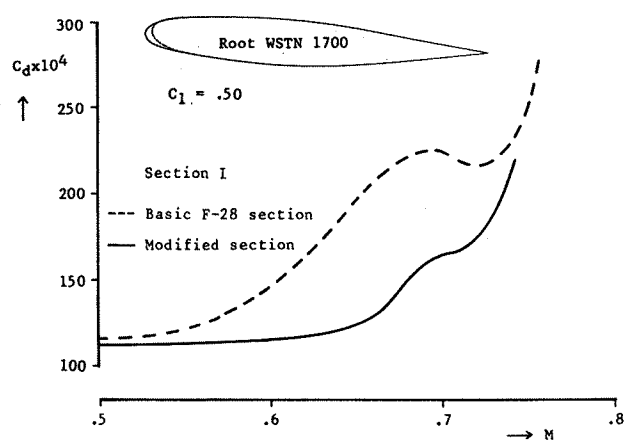
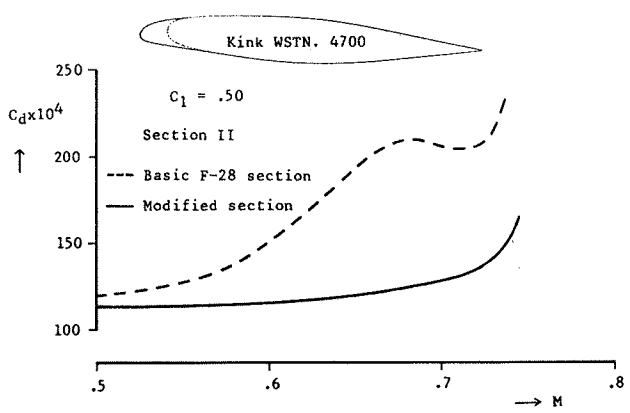
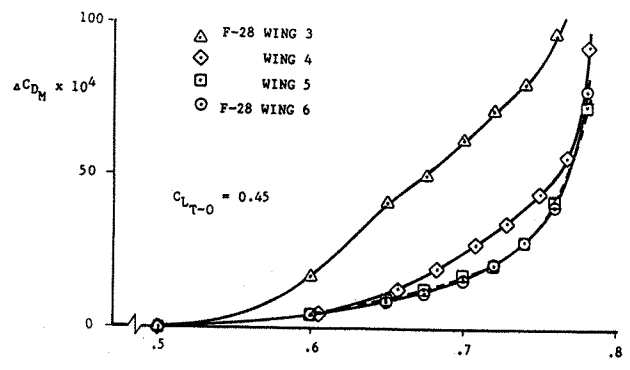


Figure 3. Noise Footprint

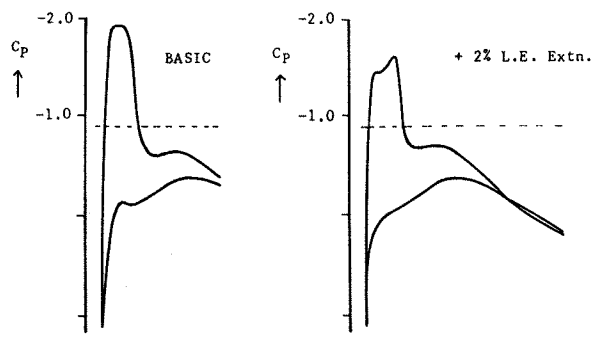


**Figure 4** Effect of modifications to root and kink sections of the F-28 wing.



**Figure 6** Mach drag rise characteristics of wings 3, 4, 5 and 6 at  $C_{L_{T=0}} = 0.45$ .

F-28 Root Section  $C_l = .4$   $M = .675$



F-28 Kink Section  $C_l = .4$   $M = .675$

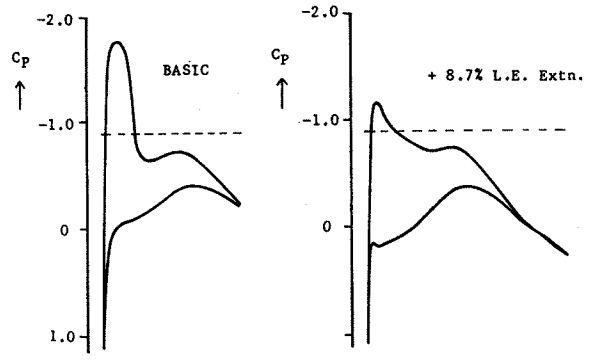


**Figure 5** Pressure distributions on basic and modified root and kink sections for the F28-wing.

F-28 Kink Section

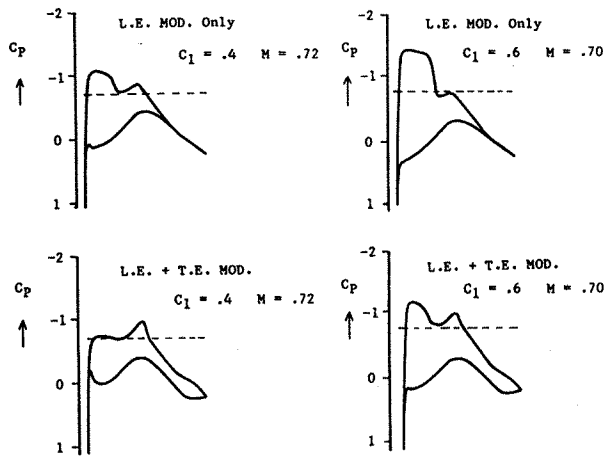
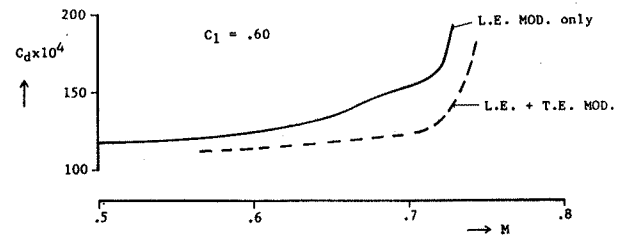


**Figure 7** Effect of trailing-edge modification on Mach-drag rise and pressure distribution.

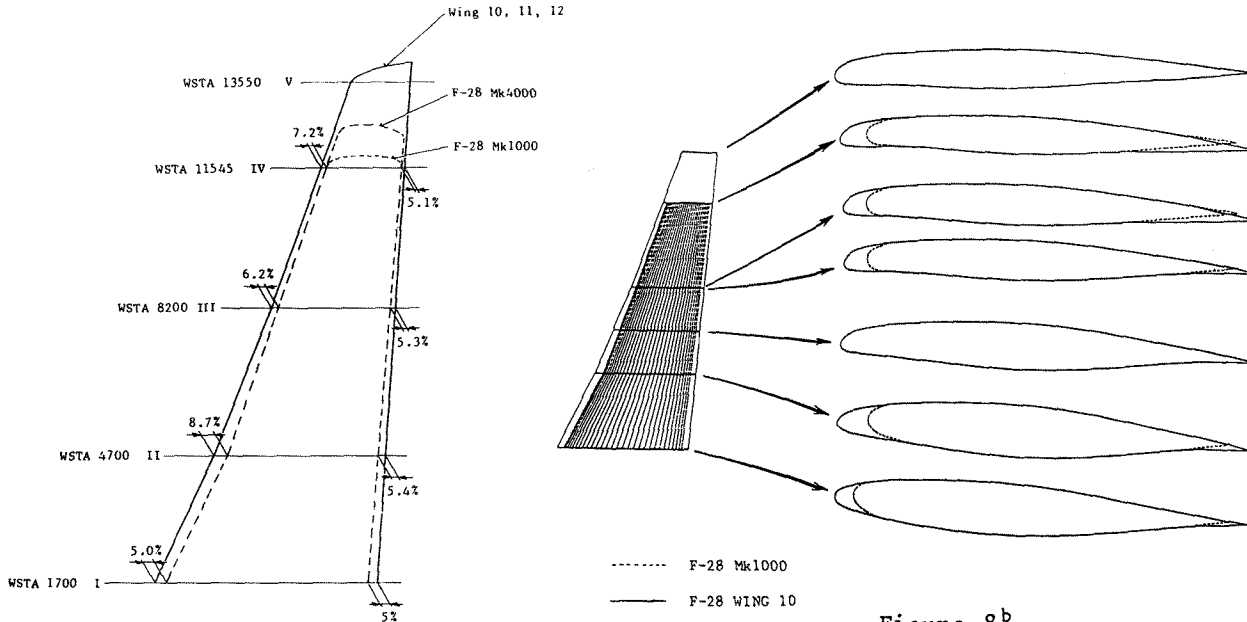


Figure 8<sup>a</sup> Comparison between F-28 and Fokker 100 wing geometry.

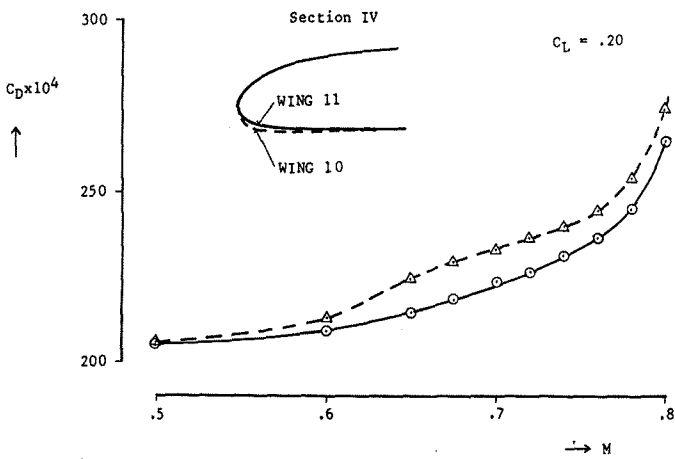


Figure 9 Effect of blunt leading-edge on the Mach drag rise at low lift coefficient.

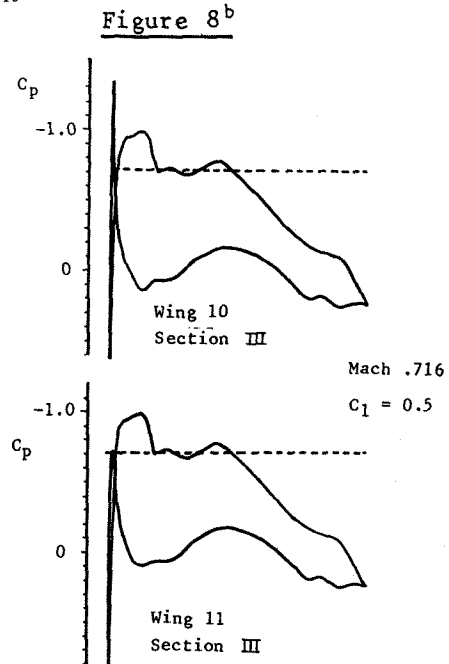


Figure 10 Effect of blunt leading-edge on the lower-surface leading-edge suction peak.

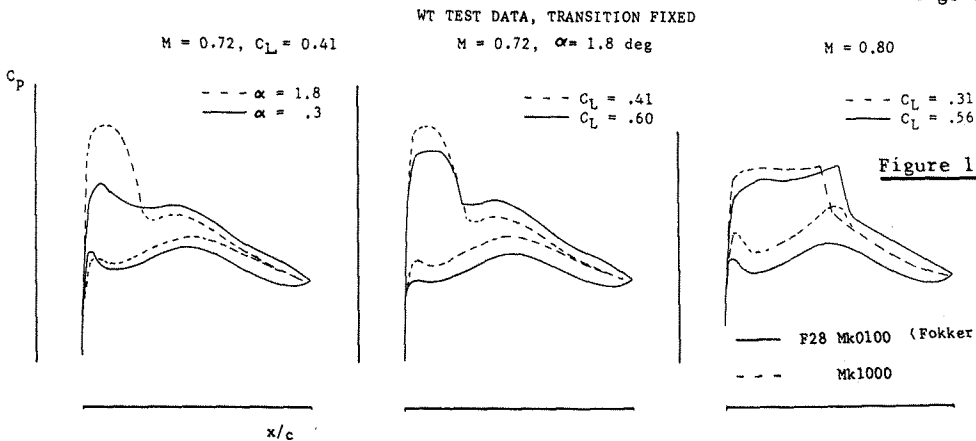


Figure 11. Comparison between the pressure distribution at a particular wing station on the F-28 Mk1000 wing and the Fokker 100 wing

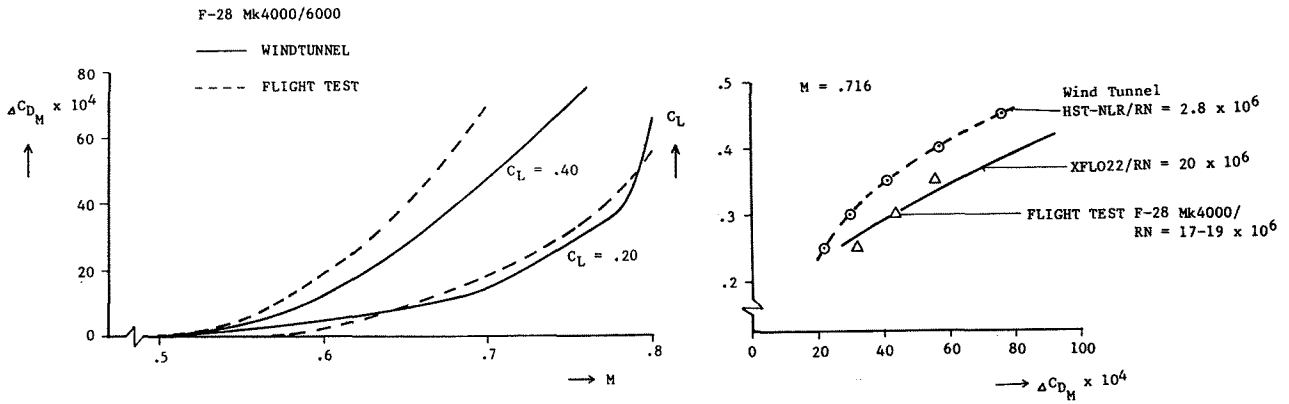


Figure 12 F-28 Comparison between Mach drag rise characteristics as measured in the wind-tunnel, in flight and as computed.

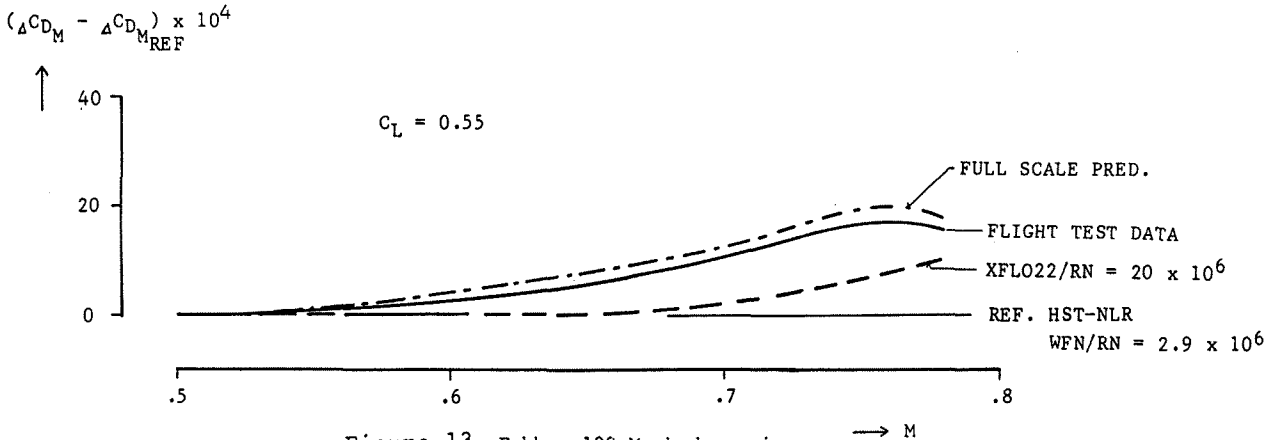


Figure 13 Fokker 100 Mach drag rise comparison between pre-flight estimate, computed and flight test data relative to wind-tunnel test data.

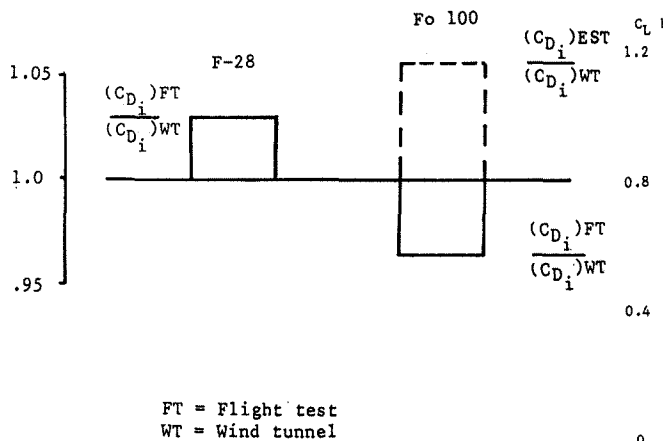


Figure 14 The induced drag as measured in flight tests compared to windtunnel data and the pre-flight estimate.

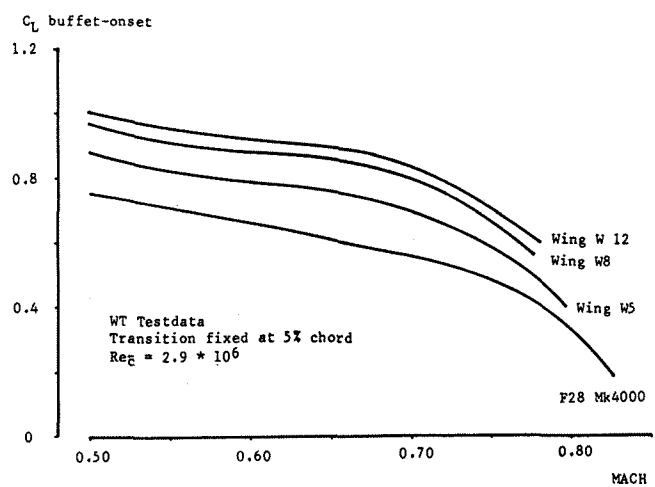


Figure 15 The development of the buffet-onset boundary

WT Test data, Transition fixed

- Complete model Wing W 12
- △ Half model

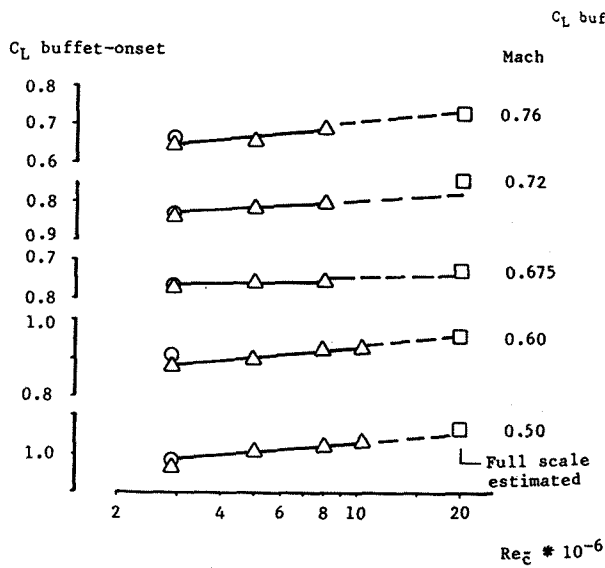


Figure 16 Estimating the full-scale buffet-onset boundary.

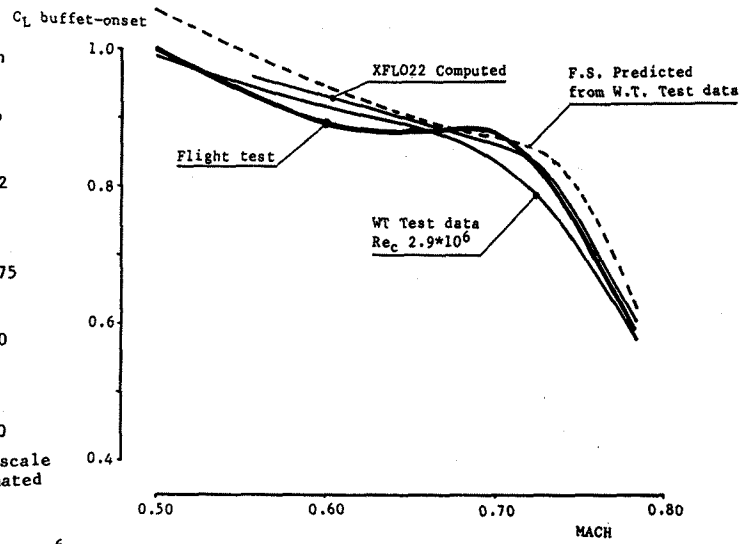
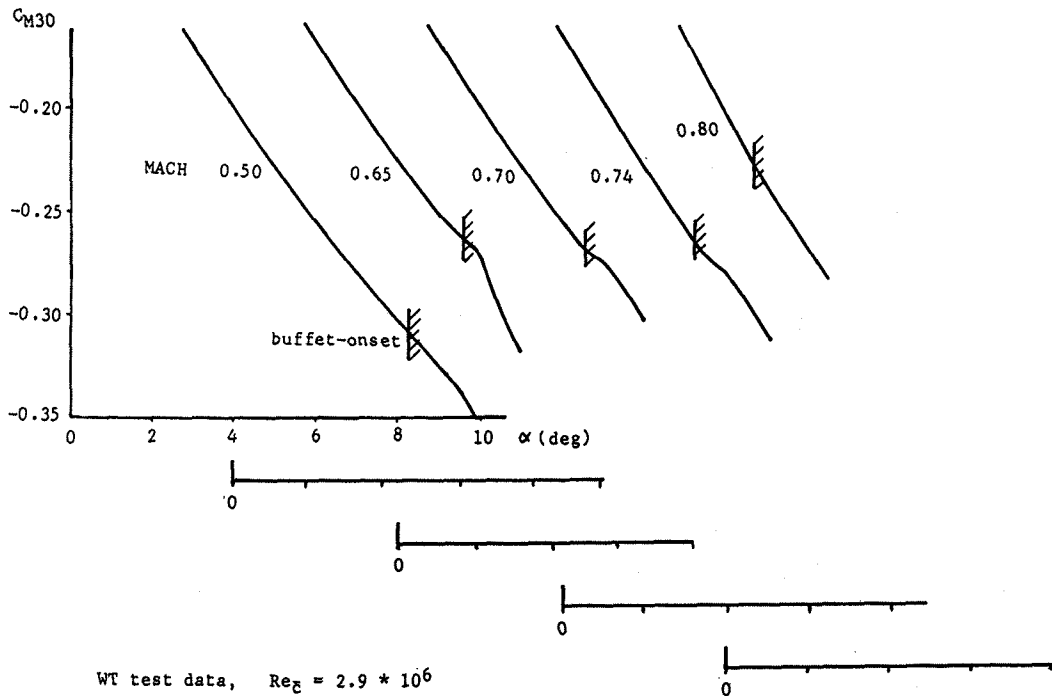
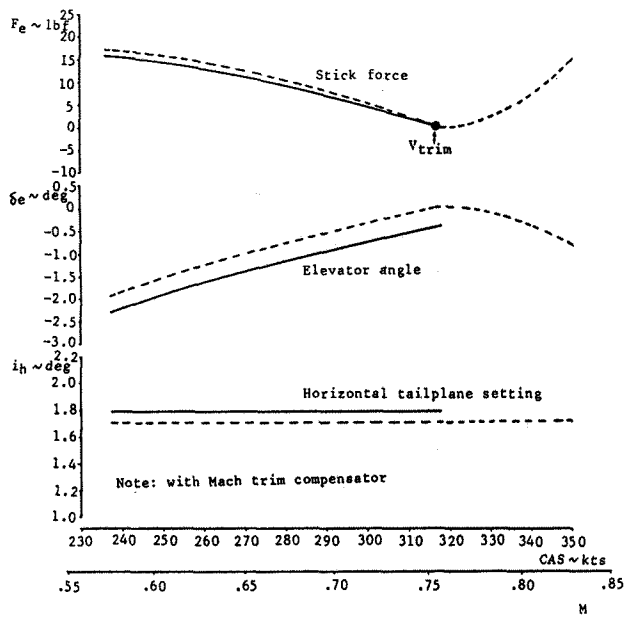


Figure 17 The full-scale buffet-onset boundary as estimated before the first flight, as computed with XFLO-22 and as derived from flight test data compared with windtunnel test data.

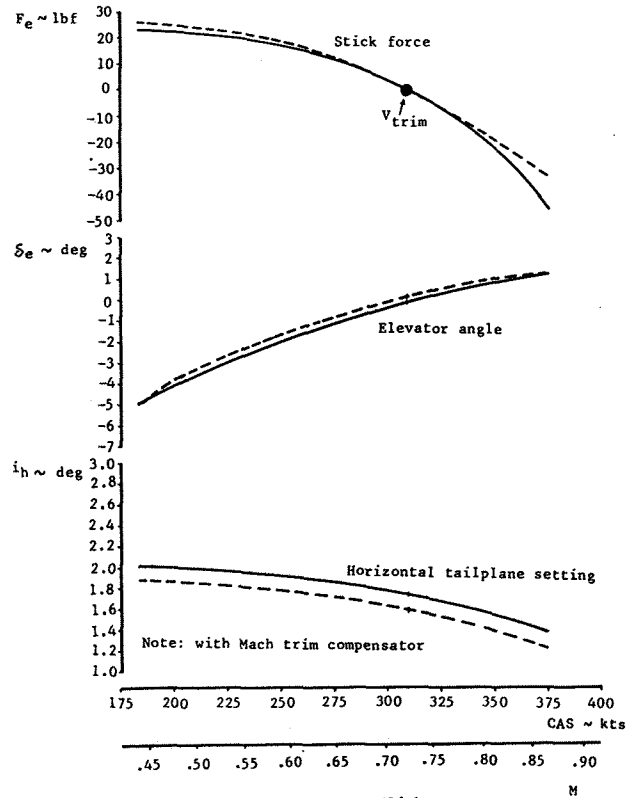


WT test data,  $Re_c = 2.9 \times 10^6$   
Transition fixed.

Figure 18 Tail-on pitching moment curves



Trimmed condition: 317 kCAS 25000ft M = 0.75  
 Configuration:  $W_e=40870$  kg c.g. 37.6% DF = 0



Trimmed condition: 310 kCAS 24000ft M.73  
 Configuration:  $W_e=41500$  kg c.g. 37.6% DF = 0

**Figure 19<sup>b</sup>** Stick force versus speed near the cruise Mach number. Mach trim compensator inoperative

**Figure 19<sup>a</sup>** Stick force versus speed near the cruise Mach number. Mach-trim compensator operative.

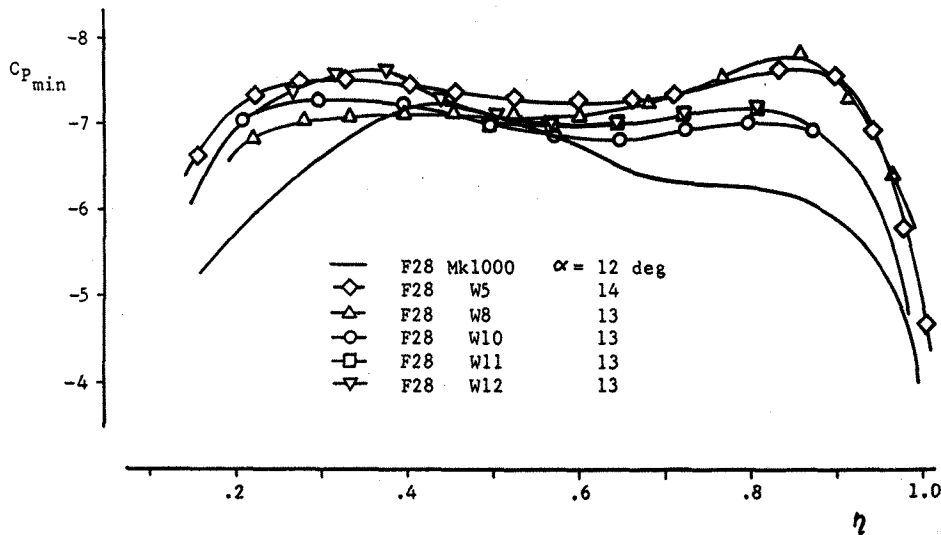


**Figure 20** The leading-edge suction peak at high angle-of-attack for successive wing designs

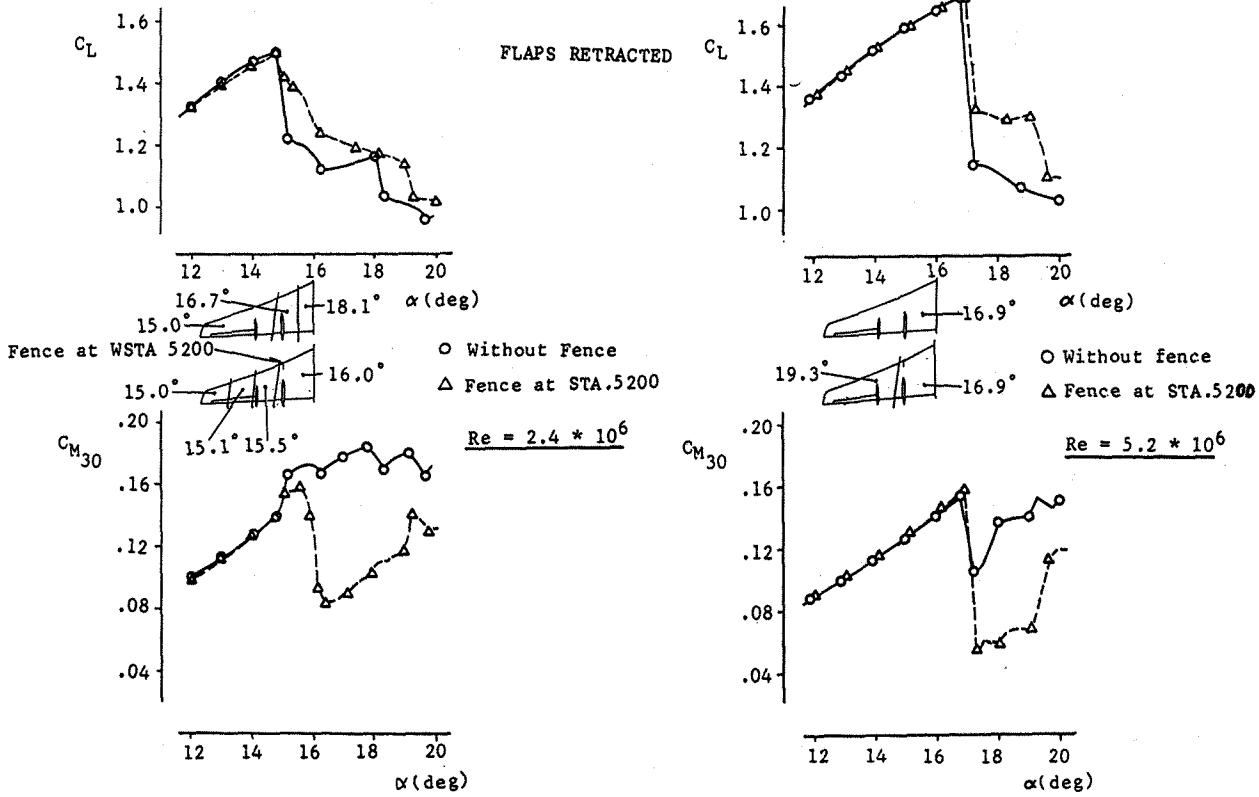


Figure 21 The effect of a leading-edge fence at WSTN 5200 on the wing stalling characteristics.

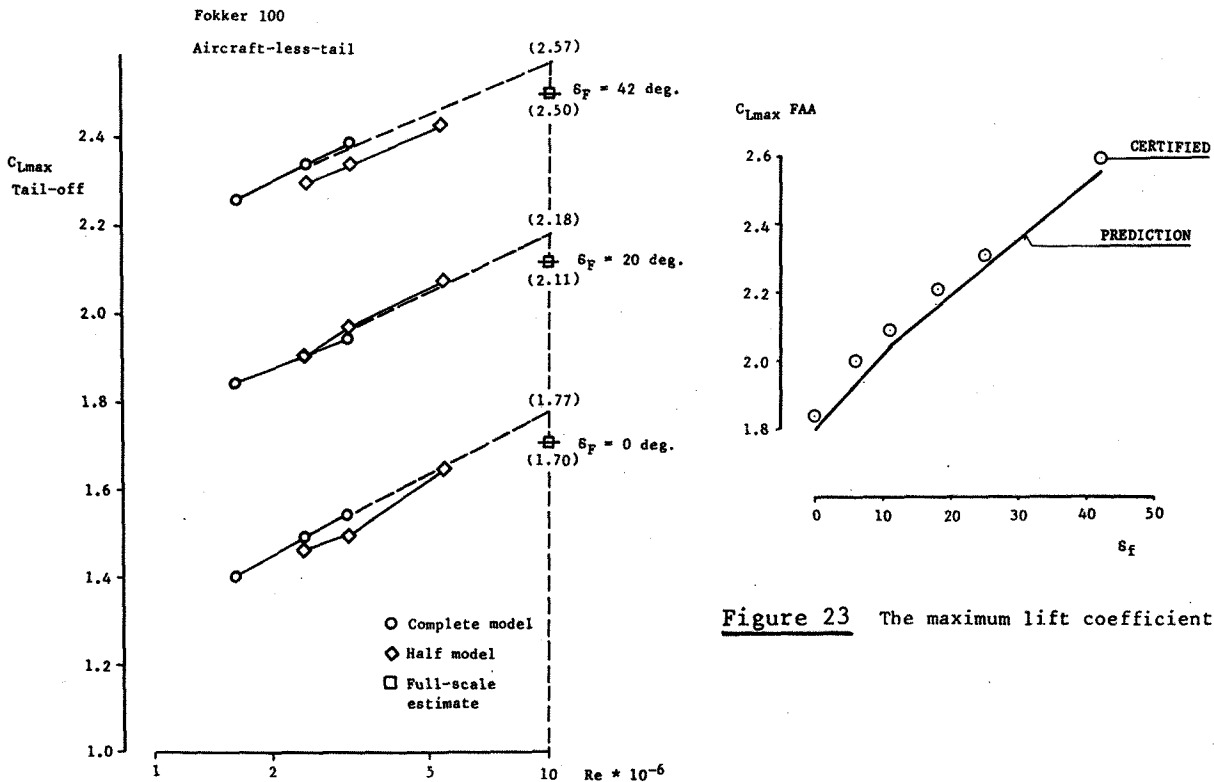
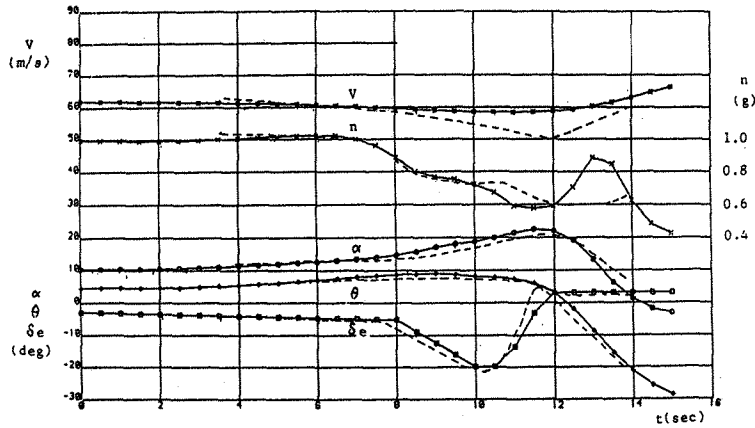


Figure 23 The maximum lift coefficient

Figure 22 The estimation of the full-scale maximum lift coefficient from windtunnel test data

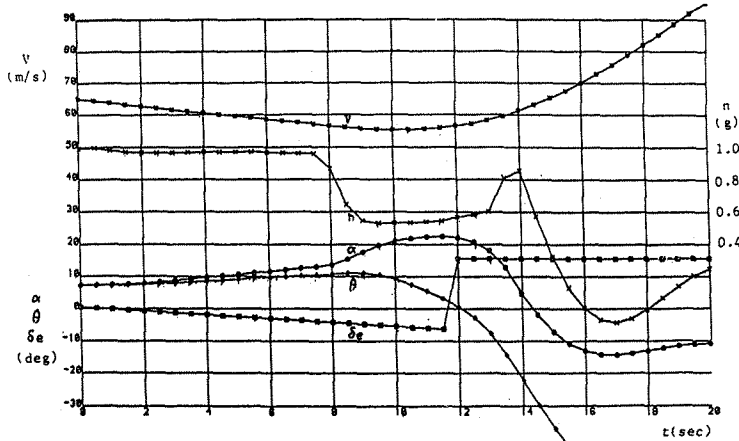


W = 29760 kgf, c.g. @ 30%,  $\delta_f = 42$  deg,  
 $\delta_{S/B} = 0$  deg

— simulator  
 - - - flight test

F28 MK 4000 FLIGHT TEST REPRODUCED

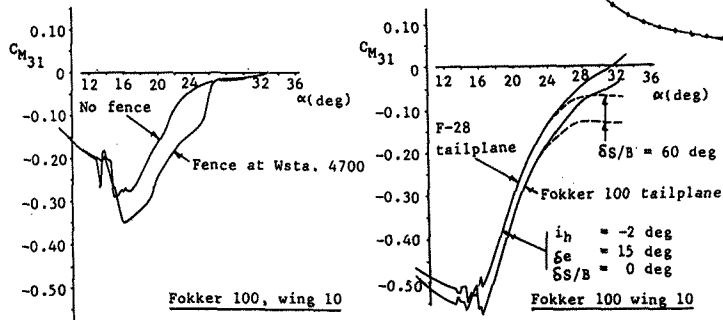
Figure 24. Stall investigation on the F-28 Mk4000



W = 33000kgf, c.g. @ 33%,  $\delta_f = 42$  deg,  
 $\delta_{S/B} = 60$  deg, push after 3 sec.

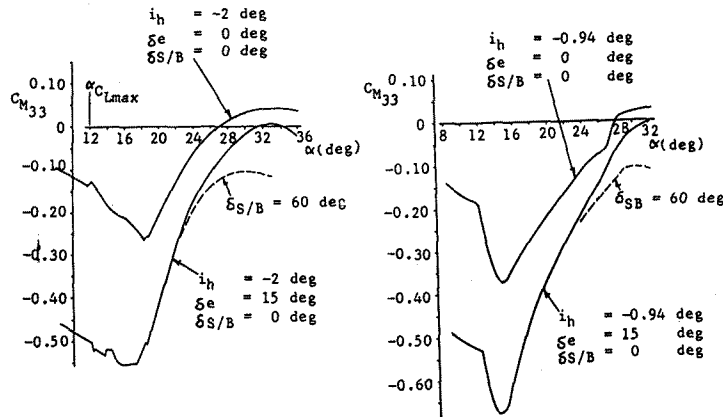
FOKKER 100 SIMULATOR DATA

Figure 25. Stall investigation on the Fokker 100 in the flight simulator



a. Effect of wing fence on pitching moment

b. Effect of tailplane span increase



c. F28 Mk4000

d. Fokker 100

Figure 26 Pitching moment at high angles-of-attack

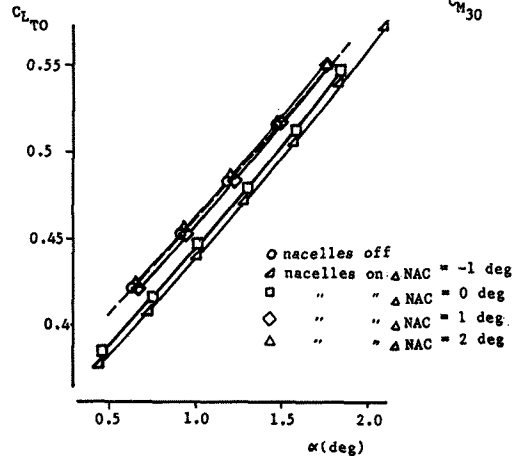
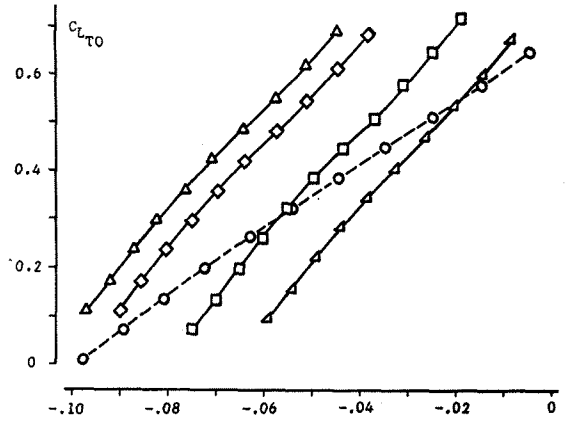


Figure 27. Effect of variations in the nacelle inclination on the tail-off lift and pitching moment



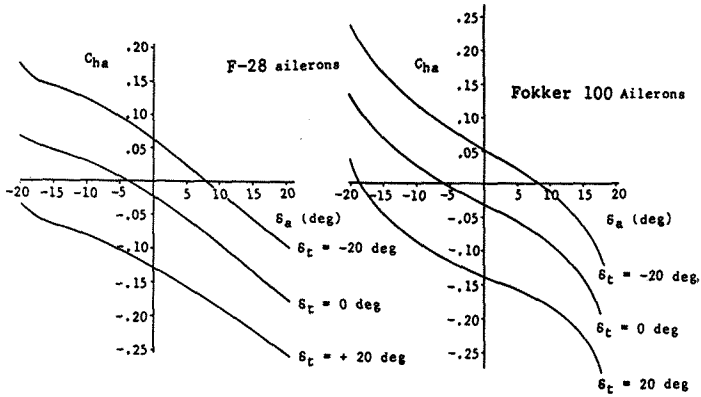


Figure 28 Aileron hinge moments

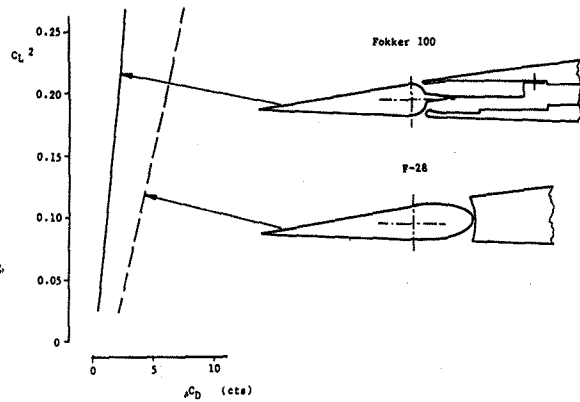


Figure 29 Effect of aileron gap on wing drag

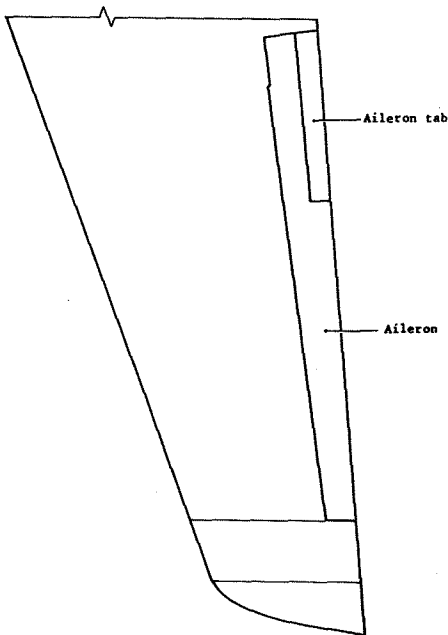


Figure 30 Fokker 100 aileron geometry

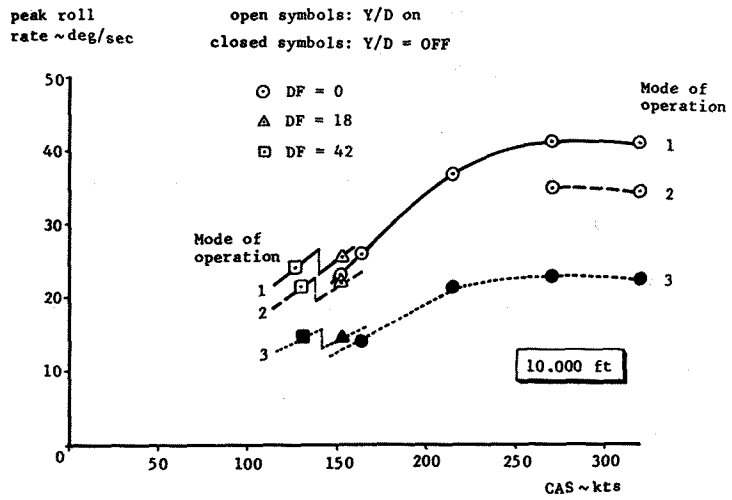


Figure 31 Fokker 100 roll performance

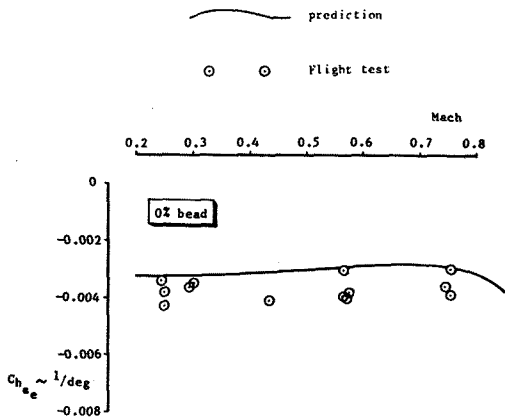


Figure 32 Elevator hinge moment coefficient

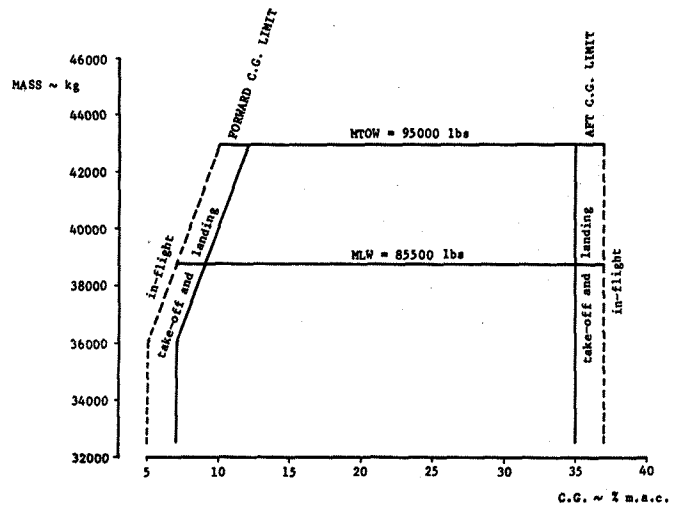
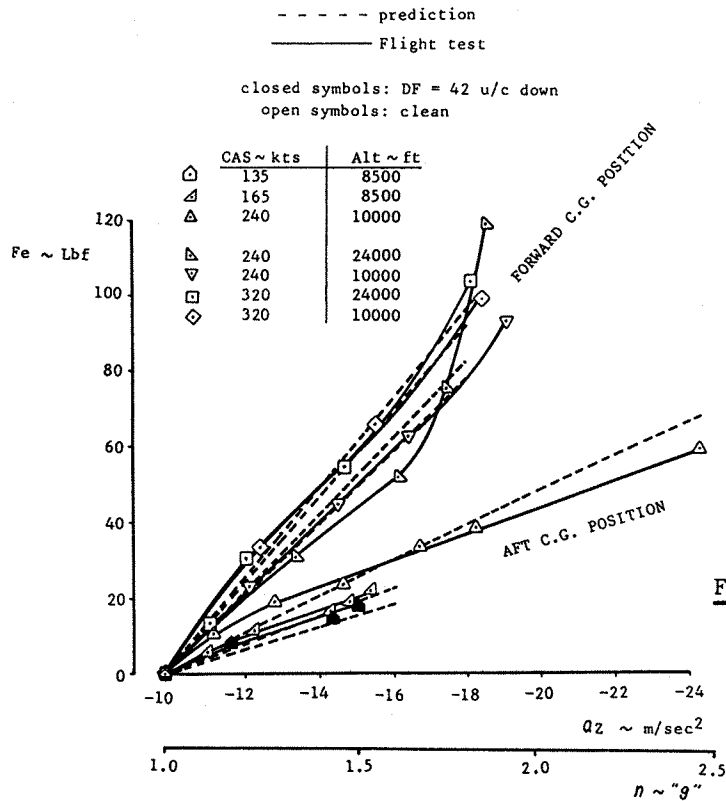
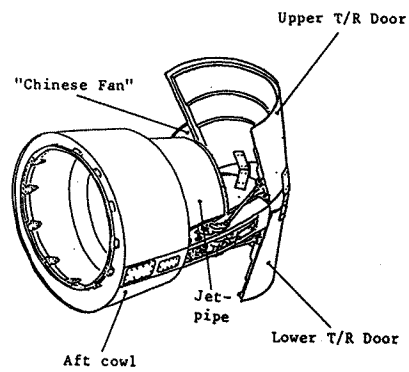


Figure 33 Fokker 100 - Loading diagram



**Figure 34** Longitudinal control force versus normal load factor



**Figure 35** Thrust reverser with "Chinese fan"

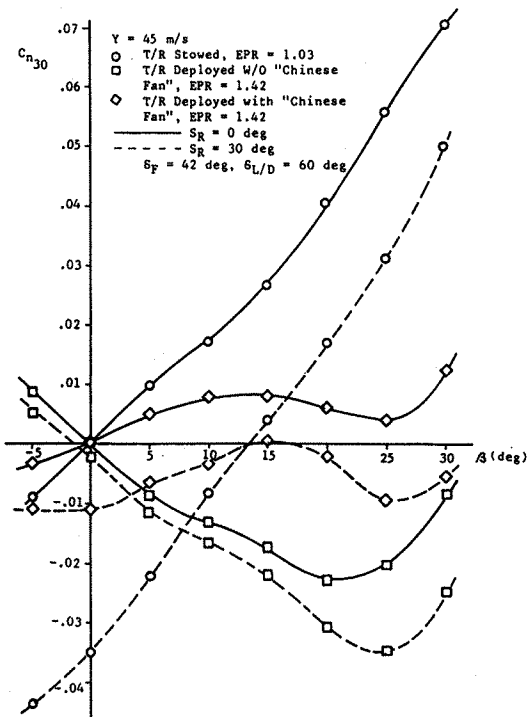


**Figure 36** The effect of the "Chinese Fan" on the directional stability and control with thrust reverser deployed.

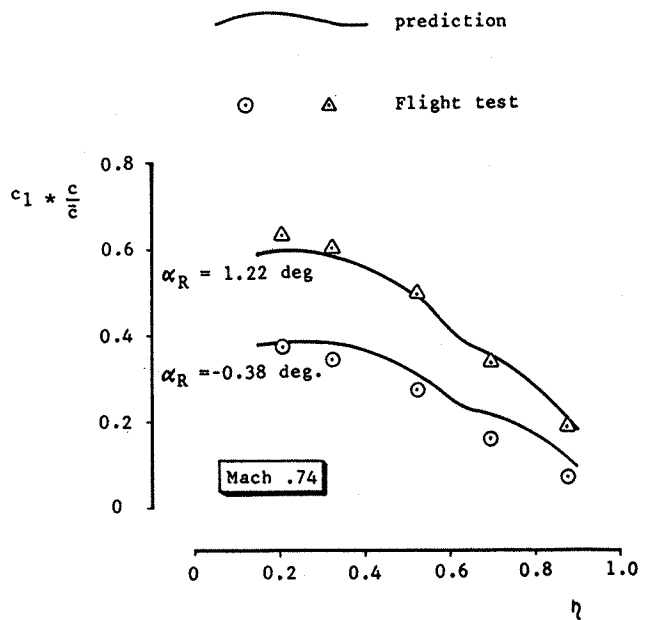


**Figure 37** Spanwise lift distribution

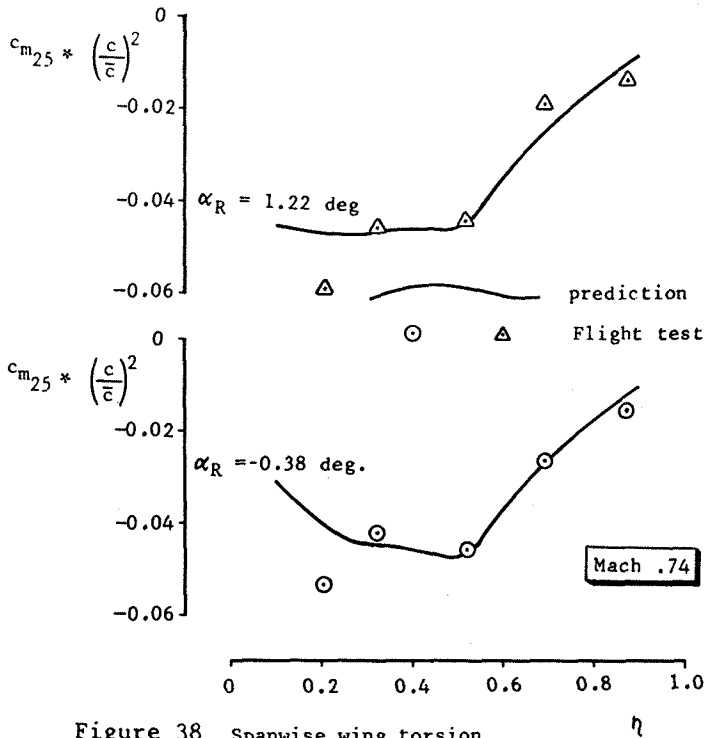


Figure 38 Spanwise wing torsion moment distribution

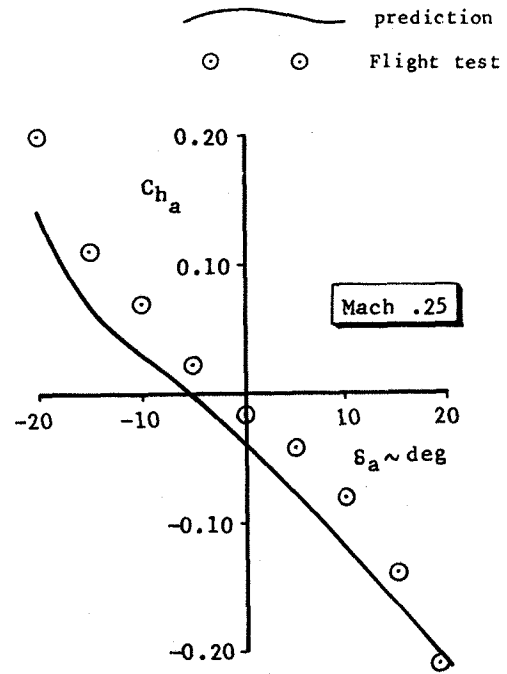


Figure 39 Aileron hinge moment

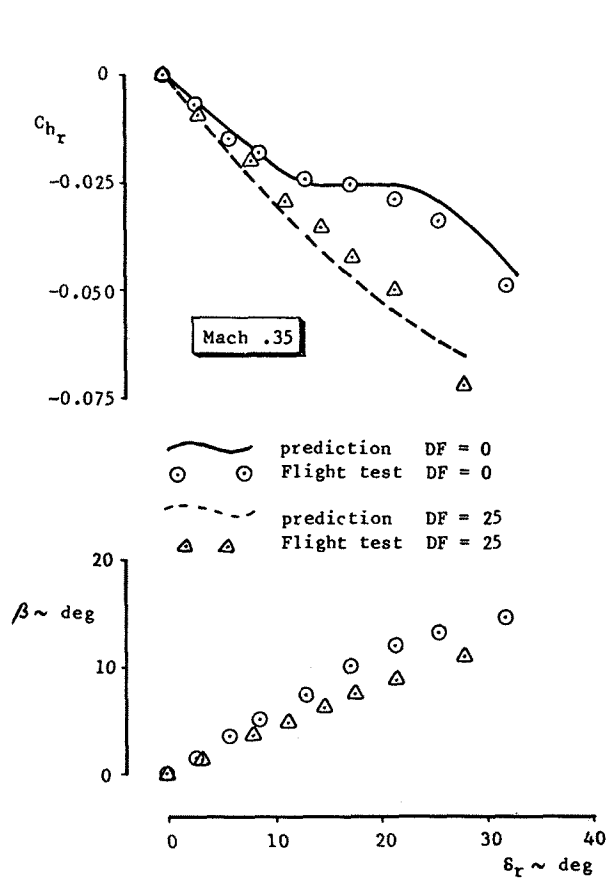


Figure 40 Rudder hinge moment

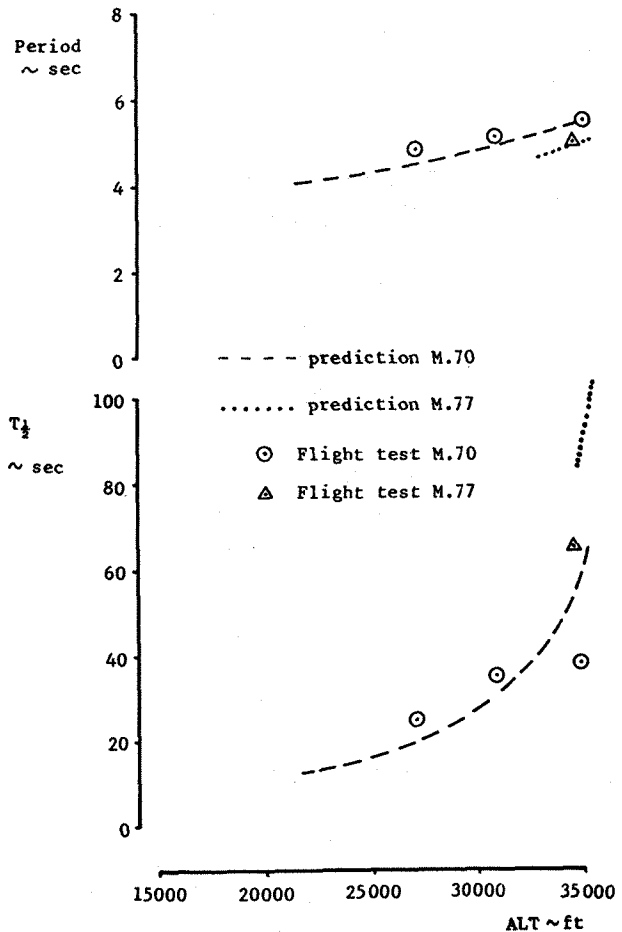


Figure 41 Dutch-roll characteristics.

## Planning vs reality

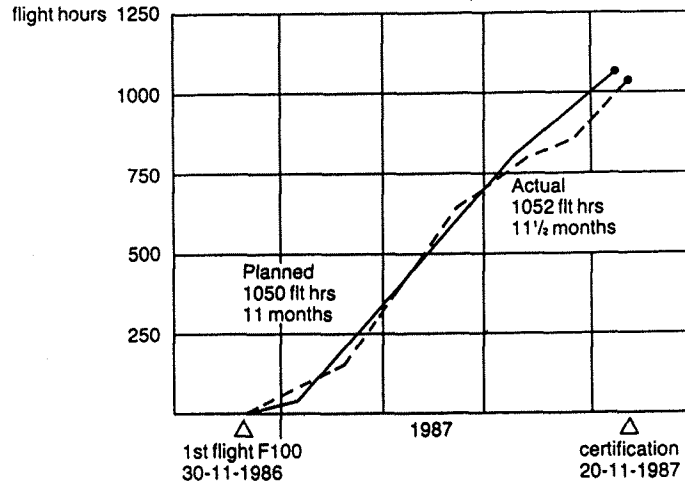


Figure 42. Flight Test Results

### Program split up (flight hours)

	planned		reality
	1983	1986	20-11-87
flight envelope	30	35	20
aero elasticity/flutter	10	10	6
flight handling	80	253	265
performance	200	228	224
propulsion, incl. APU	100	82	75
avionics	170	291	227
hydr/mech. systems	20	35	72
airconditioning & anti-icing	20	42	43
noise & vibration	130	57	80
loads	20	27	29
cockpit design	20	24	11
<b>total</b>	<b>800</b>	<b>1084</b>	<b>1052</b>

Figure 43. Flight Test Result